This article has been accepted for inclusion in a future issue of this journal. Content is final as presented, with the exception of pagination.

Memristor Circuits: Flux—Charge Analysis Method

Fernando Corinto, *Senior Member, IEEE*, and Mauro Forti

***Abstract*—Memristor-based circuits are widely exploited to realize analog and/or digital systems for a broad scope of applications (e.g., amplifiers, filters, oscillators, logic gates, and memristor as synapses). A systematic methodology is necessary to understand complex nonlinear phenomena emerging in memristor circuits. The manuscript introduces a comprehensive analysis method of memristor circuits in the flux-charge (φ, q)-domain. The proposed method relies on Kirchhoff Flux and Charge Laws and constitutive relations of circuit elements in terms of incremental flux and charge. The main advantages (over the approaches in the voltage-current (v, i)-domain) of the formulation of circuit equations in the (φ, q)-domain are: a) a simplified analysis of nonlinear dynamics and bifurcations by means of a smaller set of ODEs; b) a clear understanding of the influence of initial conditions. The straightforward application of the proposed method provides a full portrait of the nonlinear dynamics of the simplest memristor circuit made of one memristor connected to a capacitor. In addition, the concept of invariant manifolds permits to clarify how initial conditions give rise to bifurcations without parameters.**

***Index Terms*—Bifurcations without parameters, circuit analysis, circuit theory, memristor, nonlinear dynamics.**

I. Introduction and Motivation

MEMRISTOR was introduced in 1971 by Prof. L. O. Chua [1] as a theoretical two-terminal circuit element modeling electrical devices in terms of the integral of the current $i(t)$ and the integral of the voltage $v(t)$. Namely, a charge-controlled memristor is described by

$$\varphi(t) = h\left(q(t)\right) \tag{1}$$

where, following the nomenclature introduced in [2], the "voltage momentum" (aka "flux") and "current momentum" (aka "charge") are:

$$\varphi(t) = \int_{-\infty}^{t} v(\tau) d\tau \tag{2}$$

$$q(t) = \int_{-\infty}^{t} i(\tau) d\tau. \tag{3}$$

Manuscript received April 30, 2016; revised July 3, 2016; accepted July 4, 2016. The support from European Cooperation in Science and Technology "COST Action IC1401" is acknowledged. This paper was recommended by Associate Editor E. Blokhina.

F. Corinto is with the Department of Electronics and Telecommunications, Politecnico di Torino, Torino 10129, Italy (e-mail: fernando.corinto@polito.it).

M. Forti is with the Department of Information Engineering and Mathematics, University of Siena, 53100 Siena, Italy (e-mail: forti@diism.unisi.it).

Color versions of one or more of the figures in this paper are available online at http://ieeexplore.ieee.org.

Digital Object Identifier 10.1109/TCSI.2016.2590948

An equivalent form (see [2, Th. 1]) of (1) includes the Ohm's Law and an Ordinary Differential Equation (ODE)

$$\begin{aligned} v(t) &= R(q(t))i(t) \\ \frac{dq(t)}{dt} &= i(t) \end{aligned} \tag{4}$$

where $R(q) = dh(q)/dq$ is the memristance.

The duality principle allows one to introduce the flux-controlled memristor

$$q(t) = f\left(\varphi(t)\right) \tag{5}$$

that is

$$\begin{aligned} i(t) &= G\left(\varphi(t)\right)v(t) \\ \frac{d\varphi(t)}{dt} &= v(t) \end{aligned} \tag{6}$$

where $G(\varphi) = df(\varphi)/d\varphi$ is the memductance.

A complete classification of memristor devices in terms of the pairs of electrical variables $(v(t), i(t))$ and $(\varphi(t), q(t))$ is provided in [2]. One main result there reported is the unified description of memristor devices (i.e., without any regard to the technological realization), under the formalism based on voltage and current momenta. This approach makes easier to show that the memristor's pinched loop in the $(v(t), i(t))$ description represents just the specific response to a given external input (refer to [2, Figs. 2 and 4]).

In 2008 researchers at Hewlett-Packard recognized memristor features in single-devices based on a $Pt/TiO_2/Pt$ structure [3]. Such achievement has promoted research activities in memristor-based circuits and systems intended for a broad scope of applications. Recently, memristor-based circuits are widely exploited to realize analog and/or digital systems (e.g., amplifiers, filters, oscillators, logic gates, and memristor as synapses) [4]–[6]. Such applications are based on the following chief properties of memristor devices:

a) the fine-resolution programming of the memristance, tuned by the input amplitude, pulsewidth and frequency, in memristor acting as a non-volatile memory;
b) the inherent nonlinear dynamic behavior in memristor acting as a volatile memory.

For demonstration of the first feature, memristors are subject to low voltages during their operation as analog circuit elements and high voltages to program their memristance, i.e., memristors are exploited as pulse-programmable resistances. The programmability of memristance is also achieved with hybrid CMOS/memristor circuits due to the flexibility, reliability and high functionality of CMOS subsystems. Recently, memristor-based synapses are also realized combining a Resistive RAM memristor with a selector device (e.g., the building block is a crossbar array made of cells with 1-transistor/1-memristor or

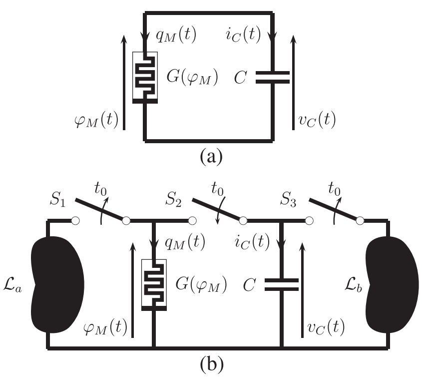

Fig. 1. The simplest memristor-based circuit. (a) $M-C$ circuit for any $t\geq t_0$. (b) $M-C$ circuit including the networks $\mathcal{L}_a$ and $\mathcal{L}_b$ that set independent initial conditions v_{C_0} and φ_{M_0} through the evolution of the electrical variables $v_C(t)$ and $\varphi_M(t)$ for $t<t_0$.

2-transistor/1-memristor) [7]. In such a case the compatibility between memristor and CMOS technologies is an issue that is still under investigation.

Nonlinear dynamic behavior of memristors is exploited in oscillatory [8], [9] and chaotic circuits [10], [11]. A thorough study is necessary to understand the rich complex nonlinear phenomena emerging in memristor circuits. Nonlinear dynamics of dual coupled memristors and of a thermally-activated locally-active memristor (based on a microstructure consisting of a bi-layer of $\mathtt{Nb_2O_5}$ and $\mathtt{Nb_2O}_x$ materials) has been investigated in [12] and [13]. Stability properties of attractors, local and global bifurcations, and the role of the initial conditions have been extensively investigated as well [14]. A systematic description (mainly based on the network theory technique referred to as the tableau method) is proposed in [15], but this leads to large systems of nonlinear Differential Algebraic Equations (DAEs), whose solution requires efficient numerical simulation tools.

The aim of the manuscript is to present a *novel systematic methodology* for the analysis of a large class of nonlinear circuits containing memristors. The class, which is denoted by $\mathcal{LM}$, is constituted by ideal capacitors, ideal inductors, ideal resistors, ideal independent voltage and current sources, and memristors that are either flux-controlled and/or charge-controlled.[1]

Any practical application of a circuit in $\mathcal{LM}$ actually starts at a *finite time instant* t_0, i.e., $-\infty<t_0<+\infty$, representing, e.g., the instant when switches are turned on or off. Given a circuit in the class $\mathcal{LM}$, with *fixed topology* for $t\geq t_0$, our goal is to develop a method to analyze its dynamics for $t\geq t_0$. An illustrative example allows us to highlight the key issues addressed by the proposed methodology and its advantages over current approaches (see in particular [8], [9], [15]).

Example: Consider the simplest memristor-based circuit in the class $\mathcal{LM}$ composed of just one memristor M connected to a capacitor C [see the $M-C$ circuit in Fig. 1(a)]. To analyze its dynamics for $t\geq t_0$ we first need to set suitable initial conditions at t_0 for the state variables $v_C(t)$ and $\varphi_M(t)$, i.e., $v_C(t_0)=v_{C_0}$ and $\varphi_M(t_0)=\varphi_{M_0}$. To this end, let us consider the circuit reported in Fig. 1(b), which is equivalent to the $M-C$ circuit for $t\geq t_0$ (i.e., S_1 and S_3 are open whereas S_2 is closed), but includes the evolution of the electrical variables $v_C(t)$ and $\varphi_M(t)$ for $t<t_0$ as well (i.e., S_1 and S_3 are closed while S_2 is open). The two-terminal circuit elements $\mathcal{L}_a$ and $\mathcal{L}_b$ can be any linear networks made of resistors, capacitors, inductors, voltage and current sources.

It is clear that we can set *independent initial conditions* v_{C_0} *and* φ_{M_0} *for the state variables* $v_C(t),\varphi_M(t)$ by means of the dynamics for $t<t_0$ of the circuits $\mathcal{L}_a-M$ (with S_1 closed), and $\mathcal{L}_b-C$ (with S_3 closed), respectively. We may assume that the elements M and C are not energized at $-\infty$, i.e., $v_C(-\infty)=0$, $\varphi_M(-\infty)=0$.

Analysis by inspection of the $M-C$ circuit permits to derive that $v_C(t)$ and $\varphi_M(t)$ obey the following *Initial Value Problem (IVP) for a second-order ODE* [obtained by (6)]:

$$C\frac{dv_C(t)}{dt}=-G\left(\varphi_M(t)\right)v_C(t) \tag{7}$$

$$\begin{aligned}\frac{d\varphi_M(t)}{dt}&=v_C(t)\\ v_C(t_0)&=v_{C_0}\\ \varphi_M(t_0)&=\varphi_{M_0}\end{aligned} \tag{8}$$

for any $t\geq t_0$, where v_{C_0}, φ_{M_0} are independent initial conditions for the state variables $v_C(t)$ and $\varphi_M(t)$ at t_0.

Note that the r.h.s. of (7) can be written as

$$-G(\varphi_M(t))v_C(t)=-\frac{df(\varphi_M)}{d\varphi_M}\frac{d\varphi_M(t)}{dt}=-\frac{d}{dt}f(\varphi_M(t)) \tag{9}$$

and, as a consequence, by integrating (7) over (t_0,t), where $t\geq t_0$, we obtain

$$\begin{aligned}C\left(v_C(t)-v_C(t_0)\right)&=-\left(f(\varphi_M(t))-f\left(\varphi_M(t_0)\right)\right)\\ &=-\left(q_M(t)-q_M(t_0)\right).\end{aligned} \tag{10}$$

The chief result drawn by (10) is twofold.

First, the nonlinear dynamical behavior for $t\geq t_0$ of the $M-C$ circuit is described by the following *IVP for a first-order ODE* [derived from (10) and (8)]:

$$\begin{aligned}\frac{d\varphi_M(t)}{dt}&=-\frac{f\left(\varphi_M(t)\right)}{C}+\frac{f(\varphi_{M_0})}{C}+v_{C_0}\\ \varphi_M(t_0)&=\varphi_{M_0}\end{aligned} \tag{11}$$

where the state variable is $\varphi_M(t)$ and the initial conditions v_{C_0} and φ_{M_0} appear as constant inputs in the r.h.s.

It turns out that *the IVP* (7), (8) *for a second-order ODE in the voltage-current* (v,i)*-domain can be reduced to an IVP* (11) *for a first-order ODE in the flux-charge* (φ,q)*-domain where the r.h.s. depends on the initial conditions* v_{C_0} *and* φ_{M_0} *at* t_0 *for the state variables in the* (v,i)*-domain.*[2] This reduction is crucial in analyzing nonlinear dynamics and bifurcations in the $M-C$ circuit. The key electrical variable in (11) is just the flux $\varphi_M(t)$.[3] This confirms the results in [2] that the $(\varphi_M(t),q_M(t))$ are the sole electrical variables useful to characterize memristors and memristor circuits as well.

[1]The (linear) resistors, capacitors, and inductors can be either passive or active.

[2]It is worth to observe that two initial conditions have to be specified in order to completely determine the evolution of electrical variables in the $M-C$ circuit, i.e., the order of complexity of the $M-C$ circuit is two (see Theorem 5 in [1]).

[3]Similar considerations hold in circuits composed of one memristor connected to an inductor. In such a case the key variable is the charge $q_M(t)$ in the ideal charge-controlled memristor.

Second, (10)—which yields (11)—is derived from the integration of the Kirchhoff Current Law (KCL) over (t_0, t), thus it can be formulated as "the sum of the *capacitor incremental charge* $q_C(t) - q_C(t_0) = C(v_C(t) - v_C(t_0))$ and the *memristor incremental charge* $q_M(t) - q_M(t_0) = f(\varphi_M(t)) - f(\varphi_M(t_0))$ is zero."

It turns out that the fundamental step in reducing by one the number of ODEs in the IVP (7), (8) is the *integral of the KCL in* (t_0, t), referred to as KqL. The KqL states that "the algebraic sum of the *incremental charge* in a closed surface is zero" (*Charge Conservation Law*). With reference to the $M - C$ circuit in Fig. 1(a), we can rewrite (10) as follows:

$$q_C(t; t_0) + q_M(t; t_0) = 0 \tag{12}$$

where $q_C(t; t_0) = q_C(t) - q_C(t_0)$ and $q_M(t; t_0) = q_M(t) - q_M(t_0)$ are the capacitor and memristor incremental charges, respectively.

By duality we can also introduce the *integral of the Kirchhoff Voltage Law (KVL) in* (t_0, t), referred to as KφL, in terms of the *incremental fluxes* (*Flux Conservation Law*).

In conclusion, the illustrative example makes clear that the pillars of the new analysis method are:

- the use of KqL and KφL in terms of the incremental flux and charge

$$\varphi_k(t; t_0) \doteq \varphi_k(t) - \varphi_k(t_0) = \int_{t_0}^{t} v_k(\tau) d\tau \tag{13}$$

$$q_k(t; t_0) \doteq q_k(t) - q_k(t_0) = \int_{t_0}^{t} i_k(\tau) d\tau \tag{14}$$

  for any $t \geq t_0$, where $v_k(t)$ is the voltage across and $i_k(t)$ is current through any two-terminal element in $\mathcal{LM}$, respectively;
- the use of Constitutive Relations (CRs) expressed according to the same electrical variables, that is, CRs of resistors, capacitors, inductors, and memristors specified in terms of incremental charges and fluxes.

The main advantage of the proposed method is that it enables to describe memristor-based circuits in the class $\mathcal{LM}$ by means of IVPs for a reduced number of ODEs compared to current approaches available in literature (e.g., [8] and [15]). This permits to simplify the investigation of nonlinear dynamic behavior and bifurcation phenomena in memristor circuits and to make clear the influence of initial conditions. Section IV will present the application of the proposed flux-charge analysis method for a comprehensive study of nonlinear dynamics and bifurcations in the $M - C$ circuit of Fig. 1(a).

The key idea that allows us to develop the method is the conceptual difference between charge and flux defined in (2) and (3) and incremental charge and flux given in (13) and (14). The following property makes clear such concept.

Property 1: The incremental charge and flux in (13) and (14) reduce to the charge and flux in (2) and (3) if and only if $t_0 \to -\infty$, i.e., the circuit topology is invariant for any $t \in (-\infty, +\infty)$.

Property 1 follows directly from the definition of $\varphi_k(t, t_0)$ and $q_k(t, t_0)$. On the other hand, the past dynamics over $(-\infty, t_0)$ has to be considered in order to set independent initial conditions of a circuit switching its topology at the finite instant

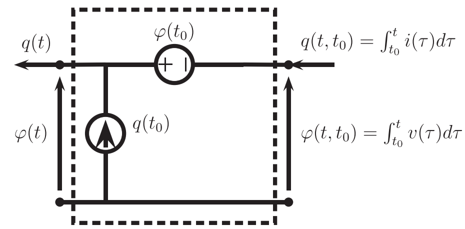

Fig. 2. Two-port network where the charge generator $q(t_0)$ and the flux generator $\varphi(t_0)$ take into account the initial conditions at a finite instant t_0.

t_0. The two-port network in Fig. 2 provides a symbolic circuit representation of (13) and (14) including a charge generator $q(t_0)$ and a flux generator $\varphi(t_0)$ to take into account initial conditions for charge and flux at t_0.

The following notation is used henceforth to denote electrical variables and parameters of any circuit in $\mathcal{LM}$. We assume the circuit has fixed topology for $t \geq t_0$ and is made of:

- n_C capacitors C_j $(j = 1, \ldots, n_C)$. The capacitor voltages $v_{C_j}(t)$ and currents $i_{C_j}(t)$ are organized in the vectors

$$\mathbf{v}_C(t) = \left(v_{C_1}(t), \ldots, v_{C_{n_C}}(t)\right)$$
$$\mathbf{i}_C(t) = \left(i_{C_1}(t), \ldots, i_{C_{n_C}}(t)\right).$$

  The corresponding incremental flux and charge vectors for $t \geq t_0$ are obtained by means of (13) and (14), that is, $\boldsymbol{\varphi}_C(t; t_0) = \boldsymbol{\varphi}_C(t) - \boldsymbol{\varphi}_C(t_0)$ and $\mathbf{q}_C(t; t_0) = \mathbf{q}_C(t) - \mathbf{q}_C(t_0)$, where

$$\boldsymbol{\varphi}_C(t) = \left(\varphi_{C_1}(t), \ldots, \varphi_{C_{n_C}}(t)\right)$$
$$\mathbf{q}_C(t) = \left(q_{C_1}(t), \ldots, q_{C_{n_C}}(t)\right).$$

- n_L inductors L_m $(m = 1, \ldots, n_L)$. The inductor voltages $v_{L_m}(t)$ and current $i_{L_m}(t)$ are organized in the vectors

$$\mathbf{v}_L(t) = \left(v_{L_1}(t), \ldots, v_{L_{n_L}}(t)\right)$$
$$\mathbf{i}_L = \left(i_{L_1}(t), \ldots, i_{L_{n_L}}(t)\right).$$

  The corresponding incremental flux and charge vectors for $t \geq t_0$ are $\boldsymbol{\varphi}_L(t; t_0) = \boldsymbol{\varphi}_L(t) - \boldsymbol{\varphi}_L(t_0)$ and $\mathbf{q}_L(t; t_0) = \mathbf{q}_L(t) - \mathbf{q}_L(t_0)$, where

$$\boldsymbol{\varphi}_L(t) = \left(\varphi_{L_1}(t), \ldots, \varphi_{L_{n_L}}(t)\right)$$
$$\mathbf{q}_L(t) = \left(q_{L_1}(t), \ldots, q_{L_{n_L}}(t)\right).$$

- n_R ideal resistors R_s $(s = 1, \ldots, n_R)$. The resistor voltages $v_{R_s}(t)$ and current $i_{R_s}(t)$ are organized as

$$\mathbf{v}_R(t) = \left(v_{R_1}(t), \ldots, v_{R_{n_R}}(t)\right)$$
$$\mathbf{i}_R = \left(i_{R_1}(t), \ldots, i_{R_{n_R}}(t)\right).$$

  The corresponding incremental flux and charge vectors for $t \geq t_0$ are $\boldsymbol{\varphi}_R(t; t_0) = \boldsymbol{\varphi}_R(t) - \boldsymbol{\varphi}_R(t_0)$ and $\mathbf{q}_R(t; t_0) = \mathbf{q}_R(t) - \mathbf{q}_R(t_0)$, where

$$\boldsymbol{\varphi}_R(t) = \left(\varphi_{R_1}(t), \ldots, \varphi_{R_{n_R}}(t)\right)$$
$$\mathbf{q}_R(t) = \left(q_{R_1}(t), \ldots, q_{R_{n_R}}(t)\right).$$

- n_M memristors M_p $(p = 1, \ldots, n_M)$. The memristor voltages $v_{M_p}(t)$ and currents $i_{M_p}(t)$ are organized as

$$\mathbf{v}_M(t) = \left(v_{M_1}(t), \ldots, v_{M_{n_M}}(t)\right)$$
$$\mathbf{i}_M = \left(i_{M_1}(t), \ldots, i_{M_{n_M}}(t)\right).$$

The corresponding incremental flux and charge vectors for $t \geq t_0$ are $\boldsymbol{\varphi}_M(t; t_0) = \boldsymbol{\varphi}_M(t) - \boldsymbol{\varphi}_M(t_0)$ and $\mathbf{q}_M(t; t_0) = \mathbf{q}_M(t) - \mathbf{q}_M(t_0)$, where

$$\boldsymbol{\varphi}_M(t) = \left(\varphi_{M_1}(t), \ldots, \varphi_{M_{n_M}}(t)\right)$$
$$\mathbf{q}_M(t) = \left(q_{M_1}(t), \ldots, q_{M_{n_M}}(t)\right).$$

- n_E ideal independent voltage sources $e_w(t)$ $(w = 1, \ldots, n_E)$. The voltages $e_w(t)$ are organized in a vector $\mathbf{e}(t) = (e_1(t), \ldots, e_{n_E}(t))$. The corresponding incremental flux vector for $t \geq t_0$ is

$$\boldsymbol{\varphi}_e(t; t_0) = \left(\varphi_{e_1}(t; t_0), \ldots, \varphi_{e_{n_E}}(t; t_0)\right).$$

- n_A ideal independent current sources $a_z(t)$ $(z = 1, \ldots, n_A)$. The currents $a_z(t)$ are organized in a vector $\mathbf{a}(t) = (a_1(t), \ldots, a_{n_A}(t))$. The corresponding incremental charge vector for $t \geq t_0$ is

$$\mathbf{q}_a(t; t_0) = \left(q_{a_1}(t; t_0), \ldots, q_{a_{n_A}}(t; t_0)\right).$$

- $\ell = n_C + n_L + n_R + n_M + n_E + n_A$ is the number of two-terminal elements $(k = 1, \ldots, \ell)$ composing any circuit in $\mathcal{LM}$. It follows that we can arrange $\mathbf{v} = (v_1, \ldots, v_\ell)'$, $\mathbf{i} = (i_1, \ldots, i_\ell)'$, $\boldsymbol{\varphi} = (\varphi_1, \ldots, \varphi_\ell)'$ and $\mathbf{q} = (q_1, \ldots, q_\ell)'$ as follows:

$$\mathbf{v}(t) = (\mathbf{v}_C(t), \mathbf{v}_L(t), \mathbf{v}_R(t), \mathbf{v}_M(t), \mathbf{v}_E(t), \mathbf{v}_A(t))'$$
$$\mathbf{i}(t) = (\mathbf{i}_C(t), \mathbf{i}_L(t), \mathbf{i}_R(t), \mathbf{i}_M(t), \mathbf{i}_E(t), \mathbf{i}_A(t))'$$
$$\boldsymbol{\varphi}(t) = (\boldsymbol{\varphi}_C(t), \boldsymbol{\varphi}_L(t), \boldsymbol{\varphi}_R(t), \boldsymbol{\varphi}_M(t), \boldsymbol{\varphi}_E(t), \boldsymbol{\varphi}_A(t))'$$
$$\mathbf{q}(t) = (\mathbf{q}_C(t), \mathbf{q}_L(t), \mathbf{q}_R(t), \mathbf{q}_M(t), \mathbf{q}_E(t), \mathbf{q}_A(t))'$$

where $(\cdot)'$ denotes the transpose vector.
- n is the number of nodes in any circuit in $\mathcal{LM}$.

II. Analysis Method in the (φ, q)-Domain

We consider in what follows a circuit in the class $\mathcal{LM}$ of nonlinear memristor circuits defined in the previous section and suppose it has a fixed topology for $t \geq t_0$, where $-\infty < t_0 < +\infty$. Our goal is to show that we can develop a method enabling to analyze the circuit dynamics for $t \geq t_0$ in the (φ, q)-domain, i.e., we can obtain circuit equations describing the dynamics no longer using the current and voltage variables. To this end we will address the following main issues:

- how to write Kirchhoff laws using the incremental charge and flux;
- how to write the CR of each element in the class $\mathcal{LM}$ and IVP for a system of ODEs in the (φ, q)-domain.

A. Incremental Kirchhoff Laws

Since ℓ is the number of two-terminal elements in $\mathcal{LM}$, and n is the number of nodes, we can write $n - 1$ fundamental cutset equations in the form $\mathbf{Ai}(t) = \mathbf{0}$ ($\mathbf{A} \in \mathbf{R}^{(n-1)\times\ell}$ is the reduced incidence matrix) and $\ell - n + 1$ fundamental loop equations $\mathbf{Bv}(t) = \mathbf{0}$ ($\mathbf{B} \in \mathbf{R}^{(\ell-n+1)\times\ell}$ is the reduced loop matrix). By integrating between t_0 and $t \geq t_0$ we obtain

$$\mathbf{Aq}(t) = \mathbf{Aq}(t_0) \tag{15}$$
$$\mathbf{B}\boldsymbol{\varphi}(t) = \mathbf{B}\boldsymbol{\varphi}(t_0). \tag{16}$$

These equations are expressed in the (φ, q)-domain and involve all the initial conditions $\mathbf{q}(t_0), \boldsymbol{\varphi}(t_0)$. It is important to stress the following key points. Among $\mathbf{q}(t_0), \boldsymbol{\varphi}(t_0)$, the initial conditions $q_{C_k}(t_0) = C_k v_{C_k}(t_0)$ and $\varphi_{L_k}(t_0) = L_k i_{L_k}(t_0)$ can be obtained *for any circuit in* $\mathcal{LM}$ by the measurement at the instant t_0 of voltages $v_{C_k}(t_0)$ across capacitors and currents $i_{L_k}(t_0)$ through inductors by means of a voltmeter or an ammeter. Instead, $q_{L_k}(t_0) = \int_{-\infty}^{t_0} i_{L_k}(t)dt$ and $\varphi_{C_k}(t_0) = \int_{-\infty}^{t_0} v_{C_k}(t)dt$ cannot be obtained via measurements at t_0 (see also footnote 11 in [16]). Rather, to evaluate $q_{L_k}(t_0)$ and $\varphi_{C_k}(t_0)$ we would require the specific knowledge of the past circuit history for $t < t_0$ [see for example Fig. 1(b)], an information that is usually unavailable or difficult to obtain in practice. In addition, it may happen that $\mathbf{q}_a(t_0)$ ($\boldsymbol{\varphi}_e(t_0)$) are not finite for some current (voltage) ideal generators.[4]

The *Kirchhoff Laws can be made independent of initial conditions* by means of the incremental fluxes and charges defined in (13) and (14). Indeed, using the incremental charge $\mathbf{q}(t, t_0)$, the Kirchhoff Charge Law (KqL) takes the simpler form

$$\mathbf{Aq}(t; t_0) = \mathbf{0} \tag{17}$$

which no longer involves the initial charges $\mathbf{q}(t_0)$, but just expresses the constraints on the incremental charges due to the topology.

Similarly, the Kirchhoff Flux Law (KφL) using the incremental flux $\boldsymbol{\varphi}(t, t_0)$ can be written as

$$\mathbf{B}\boldsymbol{\varphi}(t; t_0) = \mathbf{0}. \tag{18}$$

It is known that these equations give in overall ℓ independent topological constraints on $\mathbf{q}(t; t_0), \boldsymbol{\varphi}(t; t_0)$ in the (φ, q)-domain.

The necessity to introduce Kirchhoff Laws independent of initial conditions in turn implies that *all circuit elements have to be described by means of incremental fluxes and charges at their terminals*. The CRs of circuits elements in terms of the incremental flux and charge at their terminals are given in the next section.

Remark 1: The common assumption made in the literature to ensure that Kirchhoff Laws result to be independent of initial conditions is that $\mathbf{q}(t_0) = 0$ and $\boldsymbol{\varphi}(t_0) = 0$. This assumption is not true in general as shown in the circuit of Fig. 1(b).

[4]It is readily derived that if $a(t) = A$ ($e(t) = E$) for all $t \in (-\infty, t_0]$, with $A \in \mathbb{R}$ ($E \in \mathbb{R}$) constant, then $q_a(t_0) = \int_{-\infty}^{t_0} A d\tau$ ($\varphi_e(t_0) = \int_{-\infty}^{t_0} E d\tau$) tends to infinity.

This article has been accepted for inclusion in a future issue of this journal. Content is final as presented, with the exception of pagination.

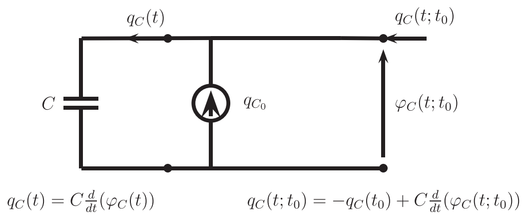

Fig. 3. Equivalent circuit for an ideal capacitor in terms of the incremental charge $q_C(t;t_0)$ and flux $\varphi_C(t;t_0)$.

B. Constitutive Relations

The discussion in Section II-A shows that it is convenient to write the KφL and KqL equations in the (φ, q)-domain by using the incremental charge $q_k(t;t_0)$ and incremental flux $\varphi_k(t;t_0)$ of each two-terminal element in $\mathcal{LM}$. Then, we are led in what follows to describe each two-terminal element by using its incremental charge $q_k(t;t_0)$ and incremental flux $\varphi_k(t;t_0)$ as port variables, i.e., to express the CR in terms of $q_k(t;t_0)$ and $\varphi_k(t;t_0)$, once appropriate reference directions are assumed at its terminals.

Next we describe in detail how to obtain CRs and equivalent circuits in the (φ, q)-domain for any two-terminal element in the class $\mathcal{LM}$ (we drop the index k to simplify the notation).

1) Ideal Capacitor: Let us consider an ideal capacitor C described by

$$q_C(t) = Cv_C(t) = C\frac{d\varphi_C(t)}{dt}.$$

Let $q_C(t_0) = q_{C_0} = Cv_C(t_0)$ be the initial charge at t_0. We obtain for $t \geq t_0$

$$q_C(t;t_0) = q_C(t) - q_C(t_0) = C\frac{d\varphi_C(t)}{dt} - Cv_C(t_0)$$

that is

$$q_C(t;t_0) = C\frac{d\varphi_C(t)}{dt} - q_{C_0}. \tag{19}$$

By noting that

$$C\frac{d\varphi_C(t)}{dt} = C\frac{d\varphi_C(t;t_0)}{dt}$$

an explicit expression of the *CR of the ideal capacitor C in terms of the incremental variables $q_C(t;t_0)$ and $\varphi_C(t;t_0)$* can be expressed as

$$q_C(t;t_0) = C\frac{d\varphi_C(t;t_0)}{dt} - q_{C_0}. \tag{20}$$

Note that this relation does not involve the electric variables (v_C, i_C). In the (φ, q)-domain the ideal capacitor C described by (20) admits of the equivalent circuit representation given in Fig. 3.[5]

2) Ideal Inductor: Let us consider an ideal inductor L described by

$$\varphi_L(t) = Li_L(t) = L\frac{dq_L(t)}{dt}.$$

[5]The circuit in Fig. 3 represents, in the (φ, q)-domain, the dual of the *initial capacitor voltage transformation* circuit reported in [17] (see Fig. 2.1 on p. 307).

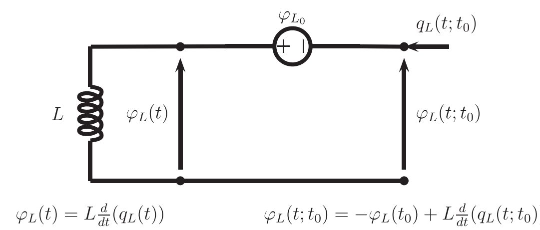

Fig. 4. Equivalent circuit for an ideal inductor in terms of the incremental charge $q_L(t;t_0)$ and flux $\varphi_L(t;t_0)$.

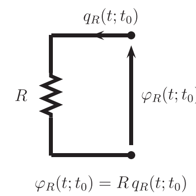

Fig. 5. Equivalent circuit for an ideal resistor in terms of the incremental charge $q_R(t;t_0)$ and flux $\varphi_R(t;t_0)$.

Following the same approach used for the ideal capacitor, we can introduce the initial flux at t_0, i.e., $\varphi_L(t_0) = \varphi_{L_0} = Li_L(t_0)$, so that:

$$\varphi_L(t;t_0) = \varphi_L(t) - \varphi_L(t_0) = L\frac{dq_L(t)}{dt} - Li_L(t_0)$$

that is

$$\varphi_L(t;t_0) = -\varphi_{L_0} + L\frac{dq_L(t)}{dt}. \tag{21}$$

By observing that

$$L\frac{dq_L(t)}{dt} = L\frac{dq_L(t;t_0)}{dt}$$

the *CR of the ideal inductor L in terms of the incremental variables $q_L(t;t_0)$ and $\varphi_L(t;t_0)$* can be expressed as

$$\varphi_L(t;t_0) = -\varphi_{L_0} + L\frac{dq_L(t;t_0)}{dt} \tag{22}$$

that corresponds to the equivalent circuit shown in Fig. 4.[6]

3) Ideal Resistor: Let us consider an ideal resistor R described by

$$v_R(t) = Ri_R(t).$$

By integrating between t_0 and $t \geq t_0$, the CR in the (φ, q)-domain results to be

$$\varphi_R(t;t_0) = Rq_R(t;t_0) \tag{23}$$

and the corresponding equivalent circuit is reported in Fig. 5. It turns out that the CR of R in the (φ, q)-domain is similar to the usual Ohm's Law because the resistor is a memoryless element.

4) Ideal Independent Voltage Source: Let us consider an ideal independent voltage source

$$v(t) = e(t) \quad \forall\, i(t)$$

[6]The circuit in Fig. 4 represents, in the (φ, q)-domain, the dual of the *initial inductor current transformation* circuit reported in [17] (see Fig. 2.1 on p. 307).

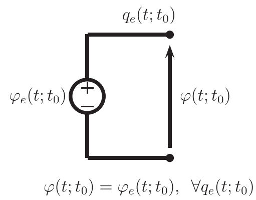

Fig. 6. Equivalent circuit for an ideal independent voltage source in terms of the incremental charge $q_e(t;t_0)$ and flux $\varphi_e(t;t_0)$.

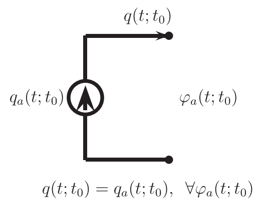

Fig. 7. Equivalent circuit for an ideal independent current source in terms of the incremental charge $q_a(t;t_0)$ and flux $\varphi_a(t;t_0)$.

where $e(t)$ is a given function of time. By integrating between t_0 and $t \geq t_0$, the CR of the ideal independent voltage source in the (φ, q)-domain can be written as

$$\varphi(t;t_0) = \varphi_e(t;t_0) \doteq \int_{t_0}^{t} e(\tau)d\tau \quad \forall\, q_e(t;t_0)$$

i.e., the incremental flux $\varphi_e(t)$ is a given function of time that is independent of the incremental charge at the generator terminals. The corresponding equivalent circuit is shown in Fig. 6.

5) Ideal Independent Current Source: Let us consider an ideal independent current source

$$i(t) = a(t) \quad \forall\, v(t)$$

where $a(t)$ is a given function of time. By integrating between t_0 and $t \geq t_0$, the CR of the ideal independent current source in the (φ, q)-domain can be written as

$$q(t;t_0) = q_a(t;t_0) \doteq \int_{t_0}^{t} a(\tau)d\tau \quad \forall\, \varphi_a(t;t_0)$$

i.e., the incremental charge $q_a(t;t_0)$ is a given function of time that is independent of the incremental voltage at the generator terminals. The corresponding equivalent circuit is shown in Fig. 7.

6) Ideal Flux-Controlled Memristor: Let us consider an ideal flux-controlled memristor

$$q_M(t) = f\left(\varphi_M(t)\right)$$

where $f(\cdot):\mathbb{R}\rightarrow\mathbb{R}$ satisfies $f(0)=0$, and let $\varphi_M(t_0)=\varphi_{M_0}$ be the initial flux of the memristor at t_0. It follows that the initial charge is $q_M(t_0)=q_{M_0}=f(\varphi_{M_0})$. By using the incremental charge and flux, the CR of the memristor M can be rewritten for $t \geq t_0$ as

$$\begin{aligned} q_M(t;t_0) &= q_M(t) - q_M(t_0) \\ &= f\left(\varphi_M(t)\right) - f\left(\varphi_M(t_0)\right) \\ &= f\left(\varphi_M(t;t_0) + \varphi_M(t_0)\right) - f\left(\varphi_M(t_0)\right). \end{aligned}$$

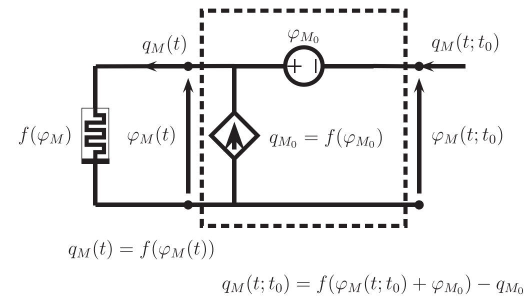

Fig. 8. Equivalent circuit for an ideal flux-controlled memristor in terms of the incremental charge $q_M(t;t_0)$ and flux $\varphi_M(t;t_0)$. The two charge and flux generators depend only on the initial flux $\varphi_M(t_0) = \varphi_{M_0}$.

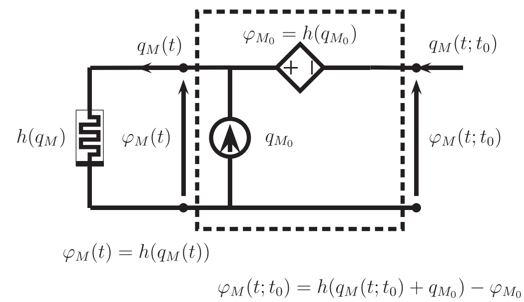

Fig. 9. Equivalent circuit for an ideal charge-controlled memristor in terms of the incremental charge $q_M(t;t_0)$ and flux $\varphi_M(t;t_0)$. The two charge and flux generators depend only on the initial charge $q_M(t_0) = q_{M_0}$.

As a consequence, the *CR of the ideal memristor M in terms of the incremental variables $q_M(t;t_0)$ and $\varphi_M(t;t_0)$* is

$$q_M(t;t_0) = f\left(\varphi_M(t;t_0) + \varphi_{M_0}\right) - q_{M_0}. \tag{24}$$

Note that the memristor acts as a nonlinear memoryless element in the (φ, q)-domain and its equivalent circuit is shown in Fig. 8. The equivalent circuit includes a two-port network similar to that shown in Fig. 2.

7) Ideal Charge-Controlled Memristor: Let us consider an ideal charge-controlled memristor

$$\varphi_M(t) = h\left(q_M(t)\right)$$

where $h(\cdot):\mathbb{R}\rightarrow\mathbb{R}$ satisfies $h(0) = 0$, and let $q_M(t_0) = q_{M_0}$ be the initial charge of the memristor at t_0. It follows that the initial flux is $\varphi_M(t_0) = \varphi_{M_0} = h(q_{M_0})$. By duality with respect to the flux-controlled memristor, the *CR of the ideal charge-controlled memristor M in terms of the incremental variables $q_L(t;t_0)$ and $\varphi_L(t;t_0)$* is

$$\varphi_M(t;t_0) = h(q_M\,(t;t_0) + q_{M_0}) - \varphi_{M_0} \tag{25}$$

and the corresponding equivalent circuit is in Fig. 9. The equivalent circuit includes a two-port network similar to that shown in Fig. 2.

Remark 2: Equation (25) can be obtained from (24) under the assumption that function $f(\cdot)$ is invertible, i.e., a memristor is both flux- and charge-controlled. It is also worth to observe that the class of ideal memristors includes all memristor siblings defined in [2, Th. 2] (see also [18]).

Without losing any generality, only flux-controlled memristors are considered hereinafter. All the results in the manuscript can be easily extended to circuits including either just charge-controlled memristors or flux- and charge-controlled memristors.

Remark 3: In the (φ, q)-domain memristors play the same role as nonlinear resistors in the (v, i)-domain. However, a memristor holds memory of the past history of its voltage and current through the constant generators associated to its initial condition (see Figs. 8 and 9).

Remark 4: If nonlinear resistors, capacitors and inductors are also included in the class of circuits $\mathcal{LM}$, then their piecewise-linear approximation allows us to exploit the proposed flux-charge analysis method in each interval of linearity.

Remark 5: Once each circuit element is described in the (φ, q)-domain by incremental flux and charge at its terminals, *any circuit in $\mathcal{LM}$ is obtained by connecting circuit elements using such terminals*. As a consequence, KφL and KqL result to be independent of initial conditions and provide the "usual" circuit topology constraints.

III. Formulation of the Circuit Equations

In this section the equations describing circuits in $\mathcal{LM}$ are derived by exploiting: a) the Kirchhoff laws in terms of the incremental charges and fluxes; b) the CR of each element in the class $\mathcal{LM}$. As a result, the IVP for a system of ODEs in the (φ, q)-domain is written in the form of Differential Algebraic Equations (DAEs) and State Equations (SEs).

A. Differential Algebraic Equations in the (φ, q)-Domain

Following the classical circuit analysis approach, the set of ℓ algebraic equations due to the topological constraints can be obtained by putting together the $(n-1)$ KqL-equations in (17) and the $(\ell - n + 1)$ KφL-equations in (18), that is

$$\begin{cases} \mathbf{A}\mathbf{q}(t;t_0) = \mathbf{0} \\ \mathbf{B}\boldsymbol{\varphi}(t;t_0) = \mathbf{0}. \end{cases} \tag{26}$$

The collection of all CRs, one for each of the ℓ two-terminal elements constituting a circuit in $\mathcal{LM}$, provides a set of algebraic and differential equations that can be written in terms of the incremental charge and flux as follows:

$$\begin{cases} \varphi_{R_s}(t;t_0) = R_s q_{R_s}(t;t_0), (s=1,\ldots,n_R) \\ \varphi_w(t;t_0) = \varphi_{e_w}(t;t_0) \quad \forall\, q_w(t;t_0), (w=1,\ldots,n_E) \\ q_z(t;t_0) = q_{a_z}(t;t_0) \quad \forall\, \varphi_z(t;t_0), (z=1,\ldots,n_A) \end{cases} \tag{27}$$

$$\begin{cases} C_j \frac{d\varphi_{C_j}(t;t_0)}{dt} = q_{C_j}(t;t_0) + q_{C_{j0}}, (j=1,\ldots,n_C) \\ L_m \frac{dq_{L_m}(t;t_0)}{dt} = \varphi_{L_m}(t;t_0) + \varphi_{L_{m0}}, (m=1,\ldots,n_L) \end{cases} \tag{28}$$

$$q_{M_p}(t;t_0) = f\big(\varphi_{M_p}(t;t_0) + \varphi_{M_{p0}}\big) - f(\varphi_{M_{p0}}), (p=1,\ldots,n_M). \tag{29}$$

Equations (26)–(29) provide a system of 2ℓ DAEs involving only the incremental variables $\mathbf{q}(t;t_0)$, $\boldsymbol{\varphi}(t;t_0)$. The solution of DAEs (26)–(29), with $\mathbf{q}(t_0;t_0) = \mathbf{0}$ and $\boldsymbol{\varphi}(t_0;t_0) = \mathbf{0}$, gives the evolution of $\mathbf{q}(t;t_0)$ and $\boldsymbol{\varphi}(t;t_0)$ for any $t \geq t_0$.

Remark 6: Although the DAEs (26)–(29) exploit the incremental variables in the (φ, q)-domain, their solution depends on $q_{C_{k0}}$, $\varphi_{L_{k0}}$ and $\varphi_{M_{k0}}$,[7] that is the initial conditions at t_0 for the state variables in the (v, i)-domain. Indeed, in the obtained formulation, *such initial conditions appear as constant inputs in the r.h.s. of* (28) and (29).

[7]The DAEs (26)–(29) depend also on $q_{M_{k0}}$ if charge-controlled memristors are included in the class $\mathcal{LM}$.

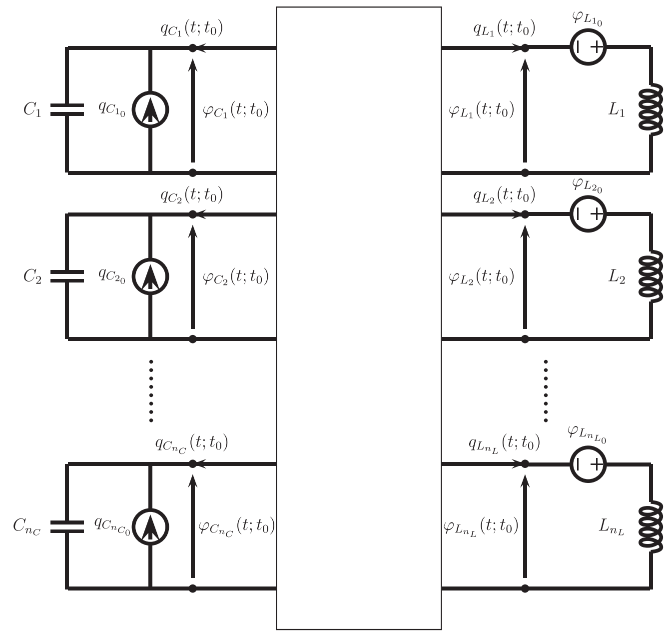

Fig. 10. Circuit representation to derive the SEs in terms of the incremental flux $\boldsymbol{\varphi}_C(t;t_0)$ and charge $\mathbf{q}_L(t;t_0)$ in the (φ, q)-domain.

B. State Equations in the (φ, q)-Domain

Circuit analysis methods based on DAEs are fundamental in numerical simulation (using, e.g., PSpice software) of linear and nonlinear circuits [15]. On the other hand, *qualitative nonlinear aspects* (e.g., the existence of no-finite-forward-escape-time solutions, eventual uniform-boundedness of solutions, local and global asymptotic stability properties, bifurcation phenomena, etc.) are more effectively analyzed by means of the SE formulation.

The formal derivation of two-common formulations and the rigorous conditions on the *existence of a global SE* representation for nonlinear RLC circuits are provided in [19]. Following the same approach as in [19], in this section the SEs in the (φ, q)-domain for any circuit in $\mathcal{LM}$ are derived. It is worth to observe that the formulation here proposed is based on $(\boldsymbol{\varphi}_C, \mathbf{q}_L)$ and is alternative to the two-common representations based on $(\mathbf{v}_C, \mathbf{i}_L)$ or $(\mathbf{q}_C, \boldsymbol{\varphi}_L)$ given in [19].

Any circuit in $\mathcal{LM}$ can be represented as shown in Fig. 10, where all capacitors and inductors are connected to an *adynamic*[8] nonlinear $(n_C + n_L)$-port including ideal resistors, memristors and ideal independent voltage and current sources.[9] Each external capacitor and inductor is represented by the equivalent circuit shown in Figs. 3 and 4, respectively. The CRs (28) describing the n_C capacitors and n_L inductors can be written in matrix form as follows:

$$\begin{cases} \mathbf{C}\frac{d}{dt}\left(\boldsymbol{\varphi}_C(t;t_0)\right) = \mathbf{q}_C(t;t_0) + \mathbf{q}_{C_0} \\ \mathbf{L}\frac{d}{dt}\left(\mathbf{q}_L(t;t_0)\right) = \boldsymbol{\varphi}_L(t;t_0) + \boldsymbol{\varphi}_{L_0} \end{cases} \tag{30}$$

[8]The term algebraic is also used in [19].

[9]The nonlinear $(n_C + n_L)$-port is adynamic because, as pointed out in Remark 3, the memristor is described by an algebraic CR in the (φ, q)-domain.

This article has been accepted for inclusion in a future issue of this journal. Content is final as presented, with the exception of pagination.

where $\mathbf{C} = \mathrm{diag}[C_1, \ldots, C_{n_C}]$ and $\mathbf{L} = \mathrm{diag}[L_1, \ldots, L_{n_L}]$ are diagonal matrices. The vectors of incremental capacitor charges $\mathbf{q}_C(t; t_0)$ and inductors fluxes $\boldsymbol{\varphi}_L(t; t_0)$ can be derived considering the adynamic nonlinear $(n_C + n_L)$-port. Under suitable assumptions, (26), (27), and (29) allow us to write (see also [19, eq. (3.9), p. 1069])

$$\begin{cases} -\mathbf{q}_C(t;t_0) = h_a(\boldsymbol{\varphi}_C(t;t_0), \mathbf{q}_L(t;t_0), \mathbf{u}(t;t_0), \boldsymbol{\varphi}_{M_0}) \\ -\boldsymbol{\varphi}_L(t;t_0) = h_b(\boldsymbol{\varphi}_C(t;t_0), \mathbf{q}_L(t;t_0), \mathbf{u}(t;t_0), \boldsymbol{\varphi}_{M_0}) \end{cases} \tag{31}$$

where $\mathbf{u}(t) = (\boldsymbol{\varphi}_E(t), \mathbf{q}_A(t))$ is the vector of fluxes and charges of the ideal independent sources. It turns out that $h_a(\cdot)$ and $h_b(\cdot)$ depend on the port-variables $(\boldsymbol{\varphi}_C, \mathbf{q}_L)$, the independent sources $\boldsymbol{\varphi}_E$, $\mathbf{q}_A$, and $\boldsymbol{\varphi}_{M_0}$, where the last term is due to initial flux of memristors[10] within the adynamic $(n_C + n_L)$-port.

By substituting (31) in (30), the following *SE formulation for $t \geq t_0$ in the (φ, q)-domain for a circuit in $\mathcal{LM}$* is obtained:

$$\begin{cases} \mathbf{C}\frac{d}{dt}\left(\boldsymbol{\varphi}_C(t;t_0)\right) = \mathbf{q}_{C_0} \\ \quad -h_a\left(\boldsymbol{\varphi}_C(t;t_0), \mathbf{q}_L(t;t_0), \mathbf{u}(t;t_0), \boldsymbol{\varphi}_{M_0}\right) \\ \mathbf{L}\frac{d}{dt}\left(\mathbf{q}_L(t;t_0)\right) = \boldsymbol{\varphi}_{L_0} \\ \quad -h_b\left(\boldsymbol{\varphi}_C(t;t_0), \mathbf{q}_L(t;t_0), \mathbf{u}(t;t_0), \boldsymbol{\varphi}_{M_0}\right) \\ \boldsymbol{\varphi}_C(t_0;t_0) = \mathbf{0} \\ \mathbf{q}_L(t_0;t_0) = \mathbf{0}. \end{cases} \tag{32}$$

Remark 7: Criteria to prove the existence of the SEs (32) and the hybrid representation (31) of the adynamic $(n_C + n_L)$-port can be derived according to the rigorous approach presented in Section III of [19] (see in particular Theorem 3 in that paper). In this manuscript the formal derivation is not reported in order to focus the readers' attention on the circuit analysis method and its applicability. We shall present the graph- and circuit-theoretic aspects in a further work.

The structure of the SEs (32) suggests the following observations:

- the state variables of the SE representation in the (φ, q)-domain are the incremental variables $\boldsymbol{\varphi}_C(t; t_0)$ and $\mathbf{q}_L(t; t_0)$;
- the evolution of the incremental variables $\boldsymbol{\varphi}_C(t; t_0)$ and $\mathbf{q}_L(t; t_0)$ is influenced by the initial conditions $\mathbf{q}_{C_0}$ and $\boldsymbol{\varphi}_{L_0}$ used in the two-common $\mathbf{v}_C - \mathbf{i}_L$ and $\mathbf{q}_C - \boldsymbol{\varphi}_L$ formulations (see point (2) in Section 3.1. of [19]) and the memristors' initial conditions $\boldsymbol{\varphi}_{M_0}$ as well. *The initial conditions $\mathbf{q}_{C_0}$, $\boldsymbol{\varphi}_{L_0}$ and $\boldsymbol{\varphi}_{M_0}$ indeed appear as constant inputs in the r.h.s. of* (32). On the other hand, the IVP for the SEs (32) has, by definition, zero initial conditions for the incremental variables $\boldsymbol{\varphi}_C(t; t_0)$ and $\mathbf{q}_L(t; t_0)$;
- the order of complexity[11] of a circuit in $\mathcal{LM}$ is $(n_C + n_L + n_M)$ if there are no constraints due to topological structures (see [1, Th. 5]).

[10]Functions $h_a(\cdot)$ and $h_b(\cdot)$ depend also on $\mathbf{q}_{M_0}$ if charge-controlled memristors are included in $\mathcal{LM}$.

[11]As reported in [1] "*The number m is called the "order of complexity" of the network and is equal to the maximum number of independent initial conditions that can be arbitrarily specified.*"

C. Differential Algebraic Equations and State Equations in the (v, i)-Domain

Given a circuit in the class $\mathcal{LM}$, the common formulation of circuit equations in the (v, i)-domain can be readily derived either by differentiating the DAEs (or SEs) in the (φ, q)-domain, or otherwise by using the KCLs, the KVLs and the CRs in terms of current and voltage. The former approach is briefly discussed in this section, whereas the latter is widely reported in the literature (see, for instance, [8]). It turns out that both methods provide the same circuit equations.

Since

$$\frac{d\mathbf{q}(t;t_0)}{dt} = \frac{d\mathbf{q}(t)}{dt} = \mathbf{i}(t)$$
$$\frac{d\boldsymbol{\varphi}(t;t_0)}{dt} = \frac{d\boldsymbol{\varphi}(t)}{dt} = \mathbf{v}(t)$$

by differentiating (26)–(28), the "usual" KCLs and KVLs

$$\begin{cases} \mathbf{A}\mathbf{i}(t) = \mathbf{0} \\ \mathbf{B}\mathbf{v}(t) = \mathbf{0} \end{cases} \tag{33}$$

are obtained. Moreover, the CRs result to be

$$\begin{cases} v_{R_s}(t) = R_s i_{R_s}(t), (s = 1, \ldots, n_R) \\ v_w(t) = e_w(t) \quad \forall\, i_w(t), (w = 1, \ldots, n_E) \\ i_z(t) = a_z(t) \quad \forall\, v_z(t), (z = 1, \ldots, n_A) \end{cases} \tag{34}$$

$$\begin{cases} C_j \frac{dv_{C_j}(t)}{dt} = i_{C_j}(t), (j = 1, \ldots, n_C) \\ L_m \frac{di_{L_m}(t)}{dt} = v_{L_m}(t), (m = 1, \ldots, n_L) \\ q_{C_j}(t_0) = q_{C_{j0}} \Rightarrow v_{C_j}(t_0) = v_{C_{j0}} \\ \varphi_{L_m}(t_0) = \varphi_{L_{m0}} \Rightarrow i_{L_m}(t_0) = i_{L_{m0}}. \end{cases} \tag{35}$$

In addition, the following CRs of memristors in the (v, i)-domain [see also (6)] are derived by differentiating (29)

$$\begin{cases} i_{M_p}(t) = G\left(\varphi_{M_p}(t)\right) v_{M_p}(t), (p = 1, \ldots, n_M) \\ \frac{d\varphi_{M_p}(t)}{dt} = v_{M_p}(t) \\ \varphi_{M_p}(t_0) = \varphi_{M_{p0}}. \end{cases} \tag{36}$$

Once the initial conditions $\mathbf{v}_C(t_0)$, $\mathbf{i}_L(t_0)$ and $\boldsymbol{\varphi}_M(t_0)$ for the state variables in the (v, i)-domain are specified, (33)–(36) provide a system of 2ℓ DAEs governing the evolution for $t \geq t_0$ of the current $\mathbf{i}(t)$ and voltage $\mathbf{v}(t)$ variables.

Noting that

$$\frac{d^2}{dt^2}\left(\boldsymbol{\varphi}_C(t;t_0)\right) = \frac{d\mathbf{v}_C(t)}{dt}$$
$$\frac{d^2}{dt^2}\left(\mathbf{q}_L(t;t_0)\right) = \frac{d\mathbf{i}_L(t)}{dt}$$

the SE formulation in the (v, i)-domain can be easily obtained by differentiating (30), that is

$$\begin{cases} \mathbf{C}\frac{d\mathbf{v}_C(t)}{dt} = \mathbf{i}_C(t) \\ \mathbf{L}\frac{d\mathbf{i}_L(t)}{dt} = \mathbf{v}_L(t) \\ \mathbf{v}_C(t_0) = \mathbf{v}_{C_0} \\ \mathbf{i}_L(t_0) = \mathbf{i}_{L_0} \end{cases} \tag{37}$$

where $\mathbf{i}_C(t)$ and $\mathbf{v}_L(t)$ can be derived by using (33), (34) and (36). In particular (36) can be written as

$$\begin{cases}\mathbf{i}_M(t) = G(\boldsymbol{\varphi}_M(t))\mathbf{v}_M(t)\\ \frac{d\boldsymbol{\varphi}_M(t)}{dt} = \mathbf{v}_M(t)\\ \boldsymbol{\varphi}_M(t_0) = \boldsymbol{\varphi}_{M_0}\end{cases} \tag{38}$$

where $\mathbf{v}_M(t)$ can be expressed in terms of $\mathbf{v}_C(t)$, $\mathbf{i}_L(t)$, $\mathbf{e}(t)$, and $\mathbf{a}(t)$, i.e.,

$$\mathbf{v}_M(t) = H_c\left(\mathbf{v}_C(t), \mathbf{i}_L(t), \mathbf{e}(t), \mathbf{a}(t)\right). \tag{39}$$

It follows that:

$$\mathbf{i}_M(t) = G\left(\boldsymbol{\varphi}_M(t)\right) H_c\left(\mathbf{v}_C(t), \mathbf{i}_L(t), \mathbf{e}(t), \mathbf{a}(t)\right)$$

and, as a consequence, $\mathbf{i}_C(t)$ and $\mathbf{v}_L(t)$ can be rewritten in the following general form[12] using (33) and (34):

$$\begin{cases}-\mathbf{i}_C(t) = H_a\left(\mathbf{v}_C(t), \mathbf{i}_L(t), \boldsymbol{\varphi}_M(t), \mathbf{e}(t), \mathbf{a}(t)\right)\\ -\mathbf{v}_L(t) = H_b\left(\mathbf{v}_C(t), \mathbf{i}_L(t), \boldsymbol{\varphi}_M(t), \mathbf{e}(t), \mathbf{a}(t)\right).\end{cases} \tag{40}$$

Finally, the IVP for the SE formulation in the (v, i)-domain is derived from (37)–(40), i.e.,

$$\begin{cases}\mathbf{C}\frac{d\mathbf{v}_C(t)}{dt} = -H_a(\mathbf{v}_C(t), \mathbf{i}_L(t), \boldsymbol{\varphi}_M(t), \mathbf{e}(t), \mathbf{a}(t))\\ \mathbf{L}\frac{d\mathbf{i}_L(t)}{dt} = -H_b(\mathbf{v}_C(t), \mathbf{i}_L(t), \boldsymbol{\varphi}_M(t), \mathbf{e}(t), \mathbf{a}(t))\\ \frac{d\boldsymbol{\varphi}_M(t)}{dt} = H_c(\mathbf{v}_C(t), \mathbf{i}_L(t), \mathbf{e}(t), \mathbf{a}(t))\\ \mathbf{v}_C(t_0) = \mathbf{v}_{C_0}\\ \mathbf{i}_L(t_0) = \mathbf{i}_{L_0}\\ \boldsymbol{\varphi}_M(t_0) = \boldsymbol{\varphi}_{M_0}.\end{cases} \tag{41}$$

It is worth to note that:

- the IVP (41) in the (v, i)-domain has n_M ODEs more than the IVP (32) in the (φ, q)-domain, i.e., *the SE formulation in the (φ, q)-domain allows us to investigate the nonlinear dynamics by means of an IVP for a smaller set of ODEs*;
- there is a one-to-one correspondence between the solution of (32)

$$\boldsymbol{\Phi}_{\varphi,q}(t, \boldsymbol{\varphi}_{C_0}, \mathbf{q}_{L_0}, \boldsymbol{\varphi}_{M_0}) = (\boldsymbol{\varphi}_C(t;t_0), \mathbf{q}_L(t;t_0))$$

and the solution of (41)

$$\boldsymbol{\Phi}_{v,i}(t, \mathbf{v}_{C_0}, \mathbf{i}_{L_0}, \boldsymbol{\varphi}_{M_0}) = (\mathbf{v}_C(t), \mathbf{i}_L(t), \boldsymbol{\varphi}_M(t))$$

expressed by the following relations:

$$\frac{d}{dt}(\boldsymbol{\varphi}_C(t;t_0)) = \mathbf{v}_C(t)$$
$$\frac{d}{dt}(\mathbf{q}_L(t;t_0)) = \mathbf{i}_L(t)$$
$$\boldsymbol{\varphi}_M(t) = \boldsymbol{\varphi}_{M_0} + \int_{t_0}^{t} H_c(\mathbf{v}_C(\tau), \mathbf{i}_L(\tau), \mathbf{e}(\tau), \mathbf{a}(\tau))\, d\tau.$$

[12]The explicit matrix representation of functions $H_a(\cdot)$, $H_b(\cdot)$, and $H_c(\cdot)$ is not essential for the presentation of the proposed circuit analysis method. By the way, we note that the examples reported in the Section IV provide a basic description of such functions.

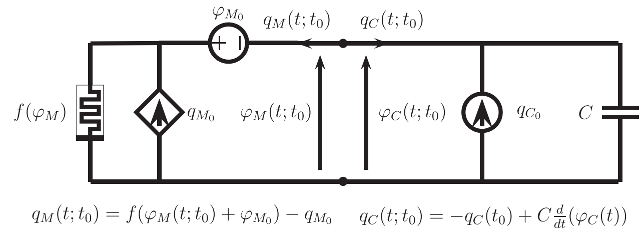

Fig. 11. Equivalent circuit in the (φ, q)-domain of the $M - C$ circuit in Fig. 1(a) for $t \geq t_0$.

IV. Nonlinear Dynamics of Memristor Circuits in the (φ, q)-Domain

This section aims at investigating the nonlinear dynamics of memristor circuits in the class $\mathcal{LM}$ by means of the SE formulation (32) in the (φ, q)-domain. Straightforward use of the equivalent circuits introduced in Section II permits to derive by inspection the circuit equations in terms of the incremental variables $\boldsymbol{\varphi}_C(t;t_0)$ and $\mathbf{q}_L(t;t_0)$. Furthermore, the concept of *invariant manifolds* is introduced to describe regions of the phase-space on which the evolution of the circuit variables takes place. The geometric structure of manifolds is crucial to unfold the bifurcation phenomena due to initial conditions (referred to as *bifurcations without parameters* [20]–[23]).

Due to lack of space, this section deals with only nonlinear dynamics and bifurcations of the $M - C$ circuit in Fig. 1(a). Memristor circuits with richer nonlinear dynamics including Hopf bifurcations (originating persistent oscillations) and period-doubling cascades (leading to chaotic behavior) shall be considered in a companion paper entitled "Memristor Circuits: Bifurcations without Parameters."

A. The Memristor-Capacitor Circuit

Let us reconsider the $M - C$ circuit in Fig. 1(a) for $t \geq t_0$.

1) Formulation of the Circuit Equations: The corresponding circuit in the (φ, q)-domain (see Fig. 11) is obtained by replacing the capacitor and the memristor with the equivalent circuits in Figs. 3 and 8, respectively. Analysis by inspection permits the direct writing of the following equations:

$$\begin{aligned} q_C(t;t_0) + q_M(t;t_0) &= 0\\ \varphi_C(t;t_0) - \varphi_M(t;t_0) &= 0\\ q_M(t;t_0) &= f(\varphi_M(t;t_0) + \varphi_{M_0}) - q_{M_0}\\ C\frac{d\varphi_C(t;t_0)}{dt} &= q_C(t;t_0) + q_{C_0}\\ \varphi_C(t_0;t_0) &= 0 \end{aligned} \tag{42}$$

where $q_{C_0} = q_C(t_0)$, $\varphi_{M_0} = \varphi_M(t_0)$, and $q_{M_0} = f(\varphi_{M_0})$. These correspond to the 2ℓ ($\ell = 2$) DAEs in (26)–(29).

The SEs in the (φ, q)-domain can be readily obtained from (42) by considering that $\varphi_C(t;t_0) = \varphi_M(t;t_0)$ and $q_C(t;t_0) = -q_M(t;t_0) = -f(\varphi_C(t;t_0) + \varphi_{M_0}) + q_{M_0}$, that is

$$\begin{cases} C\frac{d\varphi_C(t;t_0)}{dt} = -f\left(\varphi_C(t;t_0) + \varphi_{M_0}\right) + f(\varphi_{M_0}) + q_{C_0}\\ \varphi_C(t_0;t_0) = 0\end{cases} \tag{43}$$

where the initial conditions φ_{M_0} and q_{C_0} act as constant inputs.

Remark 8: The SE (43) can be put into the equivalent form reported in (11) by observing that $\varphi_C(t;t_0)=\varphi_M(t;t_0)$. It follows that $\varphi_C(t;t_0)+\varphi_{M_0}=\varphi_M(t;t_0)+\varphi_{M_0}\doteq\varphi_M(t)$ and $\varphi_C(t_0;t_0)=\varphi_M(t_0)-\varphi_{M_0}=0$. Hence, the SE (43) becomes

$$C\frac{d\varphi_M(t;t_0)}{dt}=C\frac{d\varphi_M(t)}{dt}=-f\left(\varphi_M(t)\right)+f(\varphi_{M_0})+q_{C_0}$$
$$\varphi_M(t_0)=\varphi_{M_0} \tag{44}$$

that is exactly (11) with $q_{C_0}=Cv_{C_0}$.

The common formulation of circuit equations in the (v,i)-domain can be readily derived by differentiating (42), that is

$$\begin{aligned} i_C(t)+i_M(t)&=0\\ v_C(t)-v_M(t)&=0\\ i_M(t)&=G\left(\varphi_M(t)\right)v_M(t)\\ \frac{d\varphi_M(t)}{dt}&=v_M(t)\\ C\frac{dv_c(t)}{dt}&=i_C(t) \end{aligned} \tag{45}$$

where $v_{C_0}=v_C(t_0)$ (being $q_{C_0}=q_C(t_0)$) and $\varphi_{M_0}=\varphi_M(t_0)$. These correspond to the DAEs in the (i,v)-domain in (33)–(36).

Finally, the SEs in the (v,i)-domain can be obtained by observing that $v_C(t)=v_M(t)$ implies

$$\begin{aligned} -i_C(t)&=i_M(t)=G\left(\varphi_M(t)\right)v_C(t)\\ \frac{d\varphi_M(t)}{dt}&=v_C(t) \end{aligned} \tag{46}$$

that is, functions $H_c(\cdot)$ and $H_a(\cdot)$ in (39) and (40) are

$$\begin{aligned} H_a\left(v_c(t),\varphi_M(t)\right)&=G\left(\varphi_M(t)\right)v_C(t)\\ H_c\left(v_c(t),\varphi_M(t)\right)&=v_C(t). \end{aligned} \tag{47}$$

Note that $H_b(\cdot)=0$ because there are no inductors and the dependency on $e(t)$ and $a(t)$ is not included because the circuit is autonomous.

Hence, the SE in the (v,i)-domain for the memristor-capacitor circuit results to be

$$\begin{cases} C\frac{dv_C(t)}{dt}=-G\left(\varphi_M(t)\right)v_C(t)\\ \frac{d\varphi_M(t)}{dt}=v_C(t)\\ v_C(t_0)=v_{C_0}\\ \varphi_M(t_0)=\varphi_{M_0}. \end{cases} \tag{48}$$

The IVP for the SE reported in (48) corresponds to (41) and coincides with the IVP for a second order ODE (7), (8) in the state variables $v_C(t)$ and $\varphi_M(t)$.

To summarize, the $M-C$ circuit equations have been written as SEs both in the (φ,q)-domain [see (43)] and in the (v,i)-domain [see (48)]. The two formulations are equivalent, but (43) presents a reduced number of ODEs with respect to (48). The equivalence can be easily shown under the assumption that both (43) and (48) enjoy the property of uniqueness of solutions for $t\geq t_0$. Hereinafter, we provide an explicit example in which such assumption is guaranteed. Taking into account that $\varphi_M(t;t_0)=\varphi_C(t;t_0)$, the following relationships hold true between the solutions of (43) and (48):

- if $\varphi_C(t;t_0)$ is the solution of the IVP (43) for $t\geq t_0$, then the solution of the IVP (48) can be obtained as follows:

$$\begin{aligned} v_C(t)&=\frac{d}{dt}\left(\varphi_C(t;t_0)\right)\\ \varphi_M(t)&\doteq\varphi_M(t;t_0)+\varphi_{M_0}=\varphi_C(t;t_0)+\varphi_{M_0} \end{aligned}$$

- if $(v_C(t),\varphi_M(t))$ is the solution of the IVP (48) for $t\geq t_0$, then the solution of the IVP (43) can be obtained as follows:

$$\varphi_C(t;t_0)=\varphi_M(t)-\varphi_{M_0}$$

or else

$$\varphi_C(t;t_0)\doteq\int_{t_0}^{t}v_C(\tau)d\tau.$$

2) Invariant Manifolds: The SE (43) in the (φ,q)-domain describes the evolution of the incremental flux $\varphi_C(t;t_0)$ for $t\geq t_0$ when $\varphi_C(t_0;t_0)=0$. It is important to observe that such evolution depends on the initial conditions q_{C_0} and φ_{M_0} that define the constant input $Q_0=f(\varphi_{M_0})+q_{C_0}$ in the r.h.s. of (43). The physical meaning of Q_0 is evident (by recalling $f(\varphi_{M_0})=q_{M_0}$): it represents the total charge in the $M-C$ circuit at the initial instant t_0. Let us rewrite Q_0 as follows:

$$Q_0=f\left(\varphi_M(t_0)\right)+Cv_C(t_0) \tag{49}$$

and let us introduce the *total charge* $Q(t)$ for $t\geq t_0$

$$Q(t)=f\left(\varphi_M(t)\right)+Cv_C(t). \tag{50}$$

Note that $Q(t)$ is given in terms of the state variables $v_C(t)$ and $\varphi_M(t)$ of the SE (48) in the (v,i)-domain. By definition, $Q(t_0)=Q_0$. The following property holds for the $M-C$ circuit in Fig. 11.

Property 2: The total charge $Q(t)=Q_0$ for all $t\geq t_0$.

The proof of the Property 2 is readily obtained by evaluating the time-derivative of $Q(t)$, that is

$$\frac{dQ(t)}{dt}=G\left(\varphi_M(t)\right)\frac{d\varphi_M(t)}{dt}+C\frac{dv_C(t)}{dt}=0 \tag{51}$$

due to the ODEs of the IVP (48) in the (v,i)-domain. It follows that $Q(t)$ is constant in time. Hence, $Q(t)$ keeps the initial value $Q(t_0)=Q_0$ for all $t\geq t_0$. ■

Property 2 states the physical *law of conservation of charge*, i.e., the state variables $v_C(t)$ and $\varphi_M(t)$ evolve according to (48), but the total charge $Q(t)$ remains constant to the initial value Q_0 set by v_{C_0} and φ_{M_0}. It turns out that the conservation of charge in the $M-C$ circuit follows from the KqL as well. Indeed, the first equation in (42) can be rewritten as:

$$\begin{aligned} q_C(t;t_0)+q_M(t;t_0)&=q_C(t)-q_{C_0}+q_M(t)-q_{M_0}\\ &=\left(Cv_C(t)+f\left(\varphi_M(t)\right)\right)+\\ &\quad-\left(Cv_{C_0}+f(\varphi_{M_0})\right)\\ &=Q(t)-Q(t_0)=Q(t;t_0)=0 \end{aligned} \tag{52}$$

where $Q(t,t_0)$ is the total incremental charge for $t\geq t_0$.

Property 2 permits to define an *invariant manifold* $\mathcal{M}(Q_0)$ as the region of the phase-space $(v_C, \varphi_M) \in \mathbb{R}^2$ of the SE (48) in the (v,i)-domain where $Q_0 \in \mathbb{R}$ takes a fixed value, that is

$$\mathcal{M}(Q_0) = \{(v_C, \varphi_M) \in \mathbb{R}^2 : Q(t) = Q_0 \quad \forall t \geq t_0\}. \tag{53}$$

The following observations make clear some salient features of $\mathcal{M}(Q_0)$ for the $M-C$ circuit in Fig. 11:

- *Property 3*: $\mathcal{M}(Q_0)$ is the collection of points $(v_C(t), \varphi_M(t)) \in \mathbb{R}^2$ for $t \geq t_0$ such that $f(\varphi_M(t)) + Cv_C(t) = Q_0$, i.e., it defines a one-dimensional manifold in the phase-space $\mathbb{R}^2$ of the SE (48) in the (v,i)-domain.
- *Property 4*: The uniqueness of the solution of (48) implies that there are ∞^1 one-dimensional non-intersecting manifolds $\mathcal{M}(Q_0)$, spanning the whole phase-space $\mathbb{R}^2$ of the SE (48) in the (v,i)-domain, obtained by varying Q_0 in $\mathbb{R}$.
- *Property 5*: Since $Q(t)$ is constant for any $t \geq t_0$, it follows that for any given Q_0 the manifold $\mathcal{M}(Q_0)$ is (positively) invariant for the evolution of $(v_C(t), \varphi_M(t))$, i.e., if $(v_{C_0}, \varphi_{M_0}) \in \mathcal{M}(Q_0)$ then the solution of (48) with such initial conditions belongs to $\mathcal{M}(Q_0)$ for any $t \geq t_0$. The initial charge Q_0 can be varied according to the instant t_0 in which the $M-C$ circuit changes its topology.[13]
- *Property 6*: The one-to-one correspondence between the solution of (48) and (43) implies that the dynamics on a manifold $\mathcal{M}(Q_0)$ can be also described by the SE (43) in the (φ, q)-domain. In other words, there exists a foliation of the SEs (48) in first-order dynamics on each of the ∞^1 manifolds $\mathcal{M}(Q_0)$.

3) Nonlinear Dynamics and Bifurcations: This section presents the application of the invariant manifolds concept to investigate nonlinear dynamics and bifurcations in the $M-C$ circuit of Fig. 11. Let us rewrite the SE (43) as

$$\begin{cases} C\frac{d\varphi_C(t;t_0)}{dt} = -f\left(\varphi_C(t;t_0) + \varphi_{M_0}\right) + Q_0 \\ \varphi_C(t_0;t_0) = 0 \end{cases} \tag{54}$$

where Q_0 is defined in (49). Let us assume that the CR of the memristor[14] in the $M-C$ circuit is defined by a smooth function $f(\cdot)$ that guarantees the existence and uniqueness of the solution of (54), that is

$$q_M = f(\varphi_M) = -a\varphi_M + b\varphi_M^3 \tag{55}$$

where $a, b > 0$.

Property 3 implies that the invariant manifold can be written as (for all $t \geq t_0$)

$$\mathcal{M}(Q_0) = \left\{(v_C, \varphi_M) \in \mathbb{R}^2 : v_C(t) = \frac{1}{C}\left(-f\left(\varphi_M(t)\right) + Q_0\right)\right\}. \tag{56}$$

[13]If there exist multiple instants at which the $M-C$ circuit in Fig. 1(b) switches its topology then the solution of (48) jumps across multiple manifolds.

[14]Memristors defined by the CR in (55) can be realized by a passive flux-controlled memristor (i.e., $b\varphi_M^3$) in parallel with an active resistor (i.e., a negative conductance $-a$).

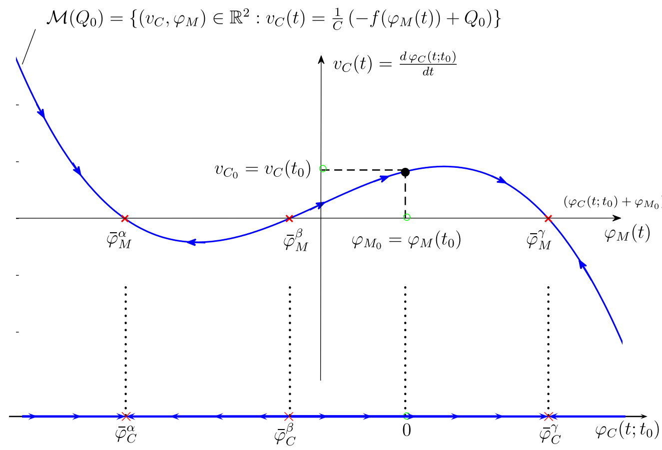

Fig. 12. Invariant manifold $\mathcal{M}(Q_0)$ and equilibrium points of (54).

By recalling that $\varphi_M(t) = \varphi_C(t;t_0) + \varphi_{M_0}$, it turns out that $\mathcal{M}(Q_0)$ is also the *dynamic route* of IVP (54), whose equilibrium points correspond to the intersection of $\mathcal{M}(Q_0)$ with $v_C = 0$ (see Fig. 12), i.e.,

$$-b\varphi_M^3 + a\varphi_M + Q_0 = 0. \tag{57}$$

The analytical solution of (57) provides the following three equilibrium points for (54):

$$\bar{\varphi}_M^\alpha = -\frac{(1+\sqrt{3}\imath)a}{\sqrt[3]{12}\sigma} - \frac{(1-\sqrt{3}\imath)\sigma}{2\sqrt[3]{18}b} \tag{58}$$

$$\bar{\varphi}_M^\beta = -\frac{(1-\sqrt{3}\imath)a}{\sqrt[3]{12}\sigma} - \frac{(1+\sqrt{3}\imath)\sigma}{2\sqrt[3]{18}b} \tag{59}$$

$$\bar{\varphi}_M^\gamma = \frac{\sqrt[3]{\frac{2}{3}}a}{\sigma} + \frac{\sigma}{\sqrt[3]{18b}} \tag{60}$$

where $\sigma = \sqrt[3]{\sqrt{3(27b^4Q_0^2 - 4a^3b^3)} + 9b^2Q_0}$. The dynamic route (see Fig. 12) permits to figure out the stability properties of equilibrium points, that is $\bar{\varphi}_M^\alpha$ and $\bar{\varphi}_M^\gamma$ are stable, whereas $\bar{\varphi}_M^\beta$ is unstable. In addition, Property 6 implies that the equilibrium points of (48) in the (v,i)-domain are the pairs $(\bar{\varphi}_M^\alpha, 0)$, $(\bar{\varphi}_M^\beta, 0)$ and $(\bar{\varphi}_M^\gamma, 0)$. Hence, in the (φ_M, v_C) phase-space any trajectory leaving from (φ_{M_0}, v_{C_0}) lies on the manifold $\mathcal{M}(Q_0)$ (see Property 5) and converges toward one of the stable equilibrium points, i.e., toward either $(\bar{\varphi}_M^\alpha, 0)$ or $(\bar{\varphi}_M^\gamma, 0)$ (the latter situation is shown in Fig. 12).

On the other hand, the dynamics in terms of the incremental flux $\varphi_C(t;t_0)$ is readily obtained by means of the relation $\varphi_M(t) = \varphi_C(t;t_0) + \varphi_{M_0}$. It follows that the equilibria of (54) are $\bar{\varphi}_M^\alpha$, $\bar{\varphi}_M^\beta$ and $\bar{\varphi}_M^\gamma$ shifted by φ_{M_0}, i.e.,

$$\bar{\varphi}_C^\alpha = \bar{\varphi}_M^\alpha - \varphi_{M_0} \tag{61}$$

$$\bar{\varphi}_C^\beta = \bar{\varphi}_M^\beta - \varphi_{M_0} \tag{62}$$

$$\bar{\varphi}_C^\gamma = \bar{\varphi}_M^\gamma - \varphi_{M_0} \tag{63}$$

and any trajectory in the one-dimensional phase-space leaving from $\varphi_C(t_0;t_0) = 0$ [see (54)] ends up in $\bar{\varphi}_C^\alpha$ or $\bar{\varphi}_C^\gamma$ (the latter situation is also shown in Fig. 12).

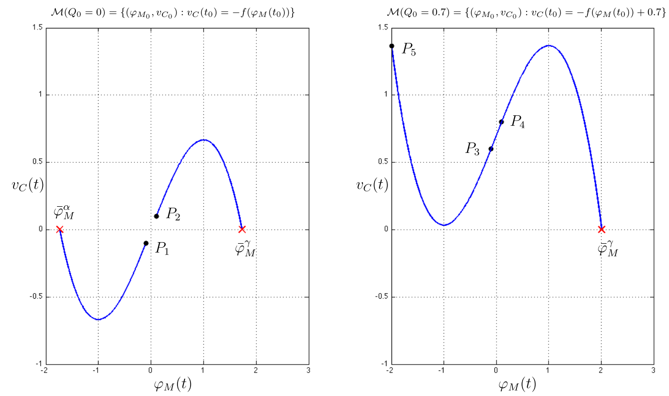

Fig. 13. Numerical simulations of the SE (48) in the (v, i)-domain with $a = 1$, $b = 1/3$ and $C = 1$. The left (resp., right) part shows the $M - C$ circuit operating in bistable mode when $Q_0 = 0$ (resp., mono-stable mode when $Q_0 = 0.7 > Q_0^{(sn)} = 2/3$). Initial conditions are: $P_1 = (0.1, -f(0.1))$, $P_2 = (-0.1, -f(-0.1))$ (i.e., $Q_0 = 0$ in P_1 and P_2), $P_3 = (0.1, -f(0.1) + 0.7)$, $P_4 = (-0.1, -f(-0.1) + 0.7)$ and $P_5 = (-2, -f(-2) + 0.7)$ (i.e., $Q_0 = 0.7$ in P_3, P_4, and P_5). The markers $\times$ correspond to stable equilibria.

The invariant manifold $\mathcal{M}(Q_0)$ permits to investigate not only equilibrium points and stability properties of (54), but bifurcation phenomena as well. It is worth to observe that, once the memristor parameters a and b are fixed, the equilibrium points (58)–(60) can move along the φ_M axis if and only if Q_0 varies. It follows that no bifurcations due to the initial conditions[15] (φ_{M_0}, v_{C_0}) occur if Q_0 is a fixed constant $\bar{Q}_0$, that is (φ_{M_0}, v_{C_0}) are such that $v_{C_0} = (1/C)(-f(\varphi_{M_0}) + \bar{Q}_0)$. This situation is referred to as *fixed invariant manifold* and the qualitative analysis of nonlinear dynamics coincides with that reported above and in Fig. 12. On the contrary, if the initial charge Q_0 is altered by the change of the topology [refer to Fig. 1(b)], then bifurcations due to initial conditions can take place. Such situation is referred to as *bifurcations without parameters* for the reason that circuit parameters are kept constant.

As regards the $M - C$ circuit described by (54), a *saddle-node bifurcation without parameters* occurs if Q_0 is such that $\bar{\varphi}_M^{\beta}$ and $\bar{\varphi}_M^{\alpha}$ (or else $\bar{\varphi}_M^{\beta}$ and $\bar{\varphi}_M^{\gamma}$) collide and annihilate each other. The conditions $\bar{\varphi}_M^{\beta} = \bar{\varphi}_M^{\alpha}$ and $\bar{\varphi}_M^{\beta} = \bar{\varphi}_M^{\gamma}$ provide

$$Q_0^{(sn)} = \pm \frac{2}{3} \frac{\sqrt[3]{a^2}}{\sqrt{3b}}. \tag{64}$$

It follows that (54) has two stable equilibrium points ($M - C$ circuit in bistable mode) for all $Q_0 \in (-|Q_0^{(sn)}|, +|Q_0^{(sn)}|)$. Otherwise it has just one equilibrium point ($M - C$ circuit in mono-stable mode). Such analytical results are also confirmed by numerical simulations (see Fig. 13) of the SE (48) in the (v, i)-domain with (dimensionless) circuit parameters: $a = 1$ and $b = 1/3$ in (55); $C = 1$.

In summary, the concept of invariant manifolds $\mathcal{M}(Q_0)$ is a powerful tool for analyzing nonlinear dynamics and bifurcations of the IVP for the SE (43) in the (φ, q)-domain. The reduced number of ODEs of the IVP in the (φ, q)-domain facilitates the analysis and permits to obtain analytical results that cannot be easily derived from the IVP (48) in the (v, i)-domain.

[15] It turns out that bifurcations can be also induced by varying the circuit parameters a, b and C.

V. Conclusion

The manuscript has introduced a comprehensive analysis method of memristor circuits in the (φ, q)-domain. The proposed method relies on Kirchhoff Flux and Charge Laws that are independent of initial conditions and constitutive relations of circuit elements in terms of incremental flux $\varphi(t; t_0)$ and charge $q(t; t_0)$. Once each circuit element is described in the (φ, q)-domain by incremental flux and charge at its terminals, any circuit in $\mathcal{LM}$ is obtained by connecting circuit elements using such terminals. The equivalent circuits in the (φ, q)-domain of resistors, capacitors, inductors, voltage and current independent source, flux-controlled and charge-controlled memristor are also provided.

The formulation of circuit equations in the (φ, q)-domain has advantages over the approach in the (v, i)-domain as it permits:

- to investigate nonlinear dynamics and bifurcations by means of an IVP for a smaller set of ODEs;
- to introduce the concept of invariant manifolds;
- to make clear the role of initial conditions in relation to bifurcations without parameters.

Remark 9: The typical approaches available in the literature to study nonlinear dynamics and bifurcations in memristor circuits make use of classical circuit analysis techniques in the (v, i)-domain. In particular, in [22] and [24] a method based on DAEs derived from the tableau analysis in the (v, i)-domain has been developed for a wide class of memristor circuits. Such method is mainly devoted to study bifurcations, and in particular bifurcations without parameters, in the specific cases where a state-variable representation in the (v, i)-domain is not available. Analytic and topological conditions for the existence of bifurcations are obtained, but the role of initial conditions in bifurcation phenomena is overlooked. Periodic oscillations and bifurcations are also investigated in a specific third-order memristor circuit by exploiting a standard state-variable description in the (v, i)-domain [20], [21]. Via geometric arguments, it is shown that there exist invariant subsets of the state space and, for fixed parameter sets, a numerical study of the bifurcations induced by varying initial conditions is conducted. Numerical studies in the (v, i)-domain on the influence of initial conditions on the dynamics and bifurcations have been carried out in [25]–[27] as well.

The straightforward application of the proposed method has enabled to thoroughly analyze the nonlinear dynamics of the simplest memristor circuit, i.e., the $M - C$ circuit introduced in Fig. 1(a). The concept of invariant manifolds, i.e., regions of the phase-space in the (v, i)-domain on which the evolution of electrical variables take place, has clarified how initial conditions give rise to bifurcations without parameters. To the best of authors' knowledge, this represents the first result that relates bifurcations without parameters with physical variables (i.e., initial conditions of dynamic circuit elements). Bifurcations without parameters in more complex circuits of the class $\mathcal{LM}$ will be reported in a companion paper entitled "Memristor Circuits: Bifurcations without parameters."

REFERENCES

[1] L. O. Chua, "Memristor-the missing circuit element," *IEEE Trans. Circuit Theory*, vol. CT-18, no. 5, pp. 507–519, 1971.

[2] F. Corinto, P. P. Civalleri, and L. O. Chua, "A theoretical approach to memristor devices," *IEEE J. Emerg. Sel. Topics Circuits Syst.*, vol. 5, no. 2, pp. 123–132, 2015.

[3] D. B. Strukov, G. S. Snider, D. R. Stewart, and R. S. Williams, "The missing memristor found," *Nature*, vol. 453, no. 7191, pp. 80–83, 2008.

[4] J. Borghetti, G. S. Snider, P. J. Kuekes, J. J. Yang, D. R. Stewart, and R. S. Williams, "Memristive switches enable stateful logic operations via material implication," *Nature*, vol. 464, no. 7290, pp. 873–876, 2010.

[5] S. Shin, K. Kim, and S.-M. Kang, "Memristor applications for programmable analog ICs," *IEEE Trans. Nanotechnol.*, vol. 10, no. 2, pp. 266–274, 2011.

[6] S. H. Jo, T. Chang, I. Ebong, B. B. Bhadviya, P. Mazumder, and W. Lu, "Nanoscale memristor device as synapse in neuromorphic systems," *Nano Lett.*, vol. 10, no. 4, pp. 1297–1301, 2010.

[7] Z. Wang, S. Ambrogio, S. Balatti, and D. Ielmini, "A 2-transistor/1-resistor artificial synapse capable of communication and stochastic learning in neuromorphic systems," *Frontiers Neurosci.*, vol. 8, p. 438, 2014.

[8] M. Itoh and L. O. Chua, "Memristor oscillators," *Int. J. Bifurcation Chaos*, vol. 18, no. 11, pp. 3183–3206, 2008.

[9] F. Corinto, A. Ascoli, and M. Gilli, "Nonlinear dynamics of memristor oscillators," *IEEE Trans. Circuits Syst. I, Reg. Papers*, vol. 58, no. 6, pp. 1323–1336, 2011.

[10] B. Muthuswamy and L. O. Chua, "Simplest chaotic circuit," *Int. J. Bifurcation Chaos*, vol. 20, no. 05, pp. 1567–1580, 2010.

[11] A. Ascoli and F. Corinto, "Memristor models in a chaotic neural circuit," *Int. J. Bifurcation Chaos*, vol. 23, no. 03, pp. 1 350 052/1–1 350 052/28, 2013.

[12] D. Yu, H. H. C. Iu, Y. Liang, T. Fernando, and L. O. Chua, "Dynamic behavior of coupled memristor circuits," *IEEE Trans. Circuits Syst. I, Reg. Papers*, vol. 62, no. 6, pp. 1607–1616, Jun. 2015.

[13] A. Ascoli, S. Slesazeck, H. Mähne, R. Tetzlaff, and T. Mikolajick, "Nonlinear dynamics of a locally-active memristor," *IEEE Trans. Circuits Syst. I, Reg. Papers*, vol. 62, no. 4, pp. 1165–1174, Apr. 2015.

[14] F. Corinto, A. Ascoli, and M. Gilli, "Analysis of current-voltage characteristics for memristive elements in pattern recognition systems," *Int. J. Circuit Theory Appl.*, vol. 40, no. 12, pp. 1277–1320, Dec. 2012.

[15] R. Riaza, "DAEs in circuit modelling: A survey," in *Surveys in Differential-Algebraic Equations I*. New York, NY, USA: Springer, 2013, pp. 97–136.

[16] L. Chua, "Device modeling via basic nonlinear circuit elements," *IEEE Trans. Circuits Syst.*, vol. CAS-27, no. 11, pp. 1014–1044, 1980.

[17] L. O. Chua, C. A. Desoer, and E. S. Kuh, *Linear and Nonlinear Circuits*. New York, NY, USA: McGraw-Hill, 1987.

[18] L. Chua, "Everything you wish to know about memristors but are afraid to ask," *Radioengineering*, vol. 24, no. 2, pp. 319–368, 2015.

[19] L. O. Chua, "Dynamic nonlinear networks: State-of-the-art," *IEEE Trans. Circuits Syst.*, vol. CAS-27, no. 11, pp. 1059–1087, 1980.

[20] M. d. C. Scarabello and M. Messias, "Bifurcations leading to nonlinear oscillations in a 3D piecewise linear memristor oscillator," *Int. J. Bifurcation Chaos*, vol. 24, no. 1, 2014, Art. no. 1430001.

[21] M. Messias, C. Nespoli, and V. A. Botta, "Hopf bifurcation from lines of equilibria without parameters in memristor oscillators," *Int. J. Bifurcation Chaos*, vol. 20, no. 2, pp. 437–450, 2010.

[22] R. Riaza, "Manifolds of equilibria and bifurcations without parameters in memristive circuits," *SIAM J. Appl. Math.*, vol. 72, no. 3, pp. 877–896, 2012.

[23] B. Fiedler, S. Liebscher, and J. C. Alexander, "Generic Hopf bifurcation from lines of equilibria without parameters: I. Theory," *J. Differential Eq.*, vol. 167, no. 1, pp. 16–35, 2000.

[24] R. Riaza and C. Tischendorf, "Semistate models of electrical circuits including memristors," *Int. J. Circuit Theory Appl.*, vol. 39, no. 6, pp. 607–627, 2011.

[25] V.-T. Pham, S. Vaidyanathan, C. Volos, S. Jafari, N. Kuznetsov, and T. Hoang, "A novel memristive time-delay chaotic system without equilibrium points," *Eur. Phys. J., Special Topics*, vol. 225, no. 1, pp. 127–136, 2016.

[26] B. Bao, Z. Ma, J. Xu, Z. Liu, and Q. Xu, "A simple memristor chaotic circuit with complex dynamics," *Int. J. Bifurcation Chaos*, vol. 21, no. 9, pp. 2629–2645, 2011.

[27] Q. Li, S. Hu, S. Tang, and G. Zeng, "Hyperchaos and horseshoe in a 4D memristive system with a line of equilibria and its implementation," *Int. J. Circuit Theory Appl.*, vol. 42, no. 11, pp. 1172–1188, 2014.

Fernando Corinto (M'03–SM'10) received the M.S. degree in electronic engineering and the Ph.D. degree in electronics and communications engineering from the Politecnico di Torino, Italy, in 2001 and 2005, respectively. He also received the European Doctorate from the Politecnico di Torino, in 2005. He was awarded a Marie Curie Fellowship in 2004.

He is currently Associate Professor of Circuit Theory with the Department of Electronics and Telecommunications, Politecnico di Torino. His research activities are mainly on nonlinear circuits and systems, locally coupled nonlinear/nanoscale networks, and memristor nanotechnology.

Prof. Corinto is coauthor of 6 book chapters and more than 120 international journal and conference papers. He is also Member of the IEEE CAS Technical Committees on "Cellular Nanoscale Networks and Array Computing" and "Nonlinear Circuits and Systems." Prof. Corinto serves as Vice-Chair of the IEEE North Italy CAS Chapter. Prof. Corinto has been an Associate Editor of the IEEE TRANSACTIONS ON CIRCUITS AND SYSTEMS—PART I: REGULAR PAPERS for 2014–2015. He is also in the Editorial Board and Review Editor of the *International Journal of Circuit Theory and Applications* since January 2015. Prof. Corinto is Vice Chair of the COST Action "Memristors—Devices, Models, Circuits, Systems and Applications (MemoCiS)." Prof. Corinto has been DRESDEN Senior Fellows at the Technische Universität Dresden in 2013. Prof. Corinto has been August-Wilhelm Scheer visiting professor at Technische Universität München in 2016 and he is also member of the Institute for Advanced Study-Technische Universität München.

Mauro Forti received the Laurea degree in electronics engineering from the University of Florence, Italy, in 1988. From 1991 to 1998, he was an Assistant Professor in applied mathematics and network theory with the Electronic Engineering Department of the University of Florence. In 1998 he joined the Department of Information Engineering of the University of Siena, Italy, where he is currently Professor of electrical engineering. His main research interests are in the field of nonlinear circuits and systems, with emphasis on the qualitative analysis and stability of circuits modeling artificial neural networks. His research activity also includes aspects of electromagnetic compatibility. Dr. Forti served as Associate Editor of the IEEE TRANSACTIONS ON CIRCUITS AND SYSTEMS I: FUNDAMENTAL THEORY AND APPLICATIONS from 2001 to 2003 and of the IEEE TRANSACTIONS ON NEURAL NETWORKS from 2001 to 2010. He is currently serving as Associate Editor of the IEEE TRANSACTIONS ON CYBERNETICS.